VLBA Imaging of NGC 4261: Symmetric Parsec-scale Jets and the Inner Accretion Region

Dayton L. Jones

Jet Propulsion Laboratory, California Institute of Technology

and

Ann E. Wehrle

Infrared Processing and Analysis Center, Jet Propulsion Laboratory,

California Institute of Technology

Received ____ ; accepted ____

ABSTRACT

Dual frequency VLBA observations of the 1111("1('11s or NGC4261(3C270) reveal highly symmetric radio structures at both 1.6 and 8.4 GHz. Analysis of these images shows that the central 10 pc of this source is not significantly affected by free-free absorption, even though the 1111(leus Of the galaxy is known to contain a nearly edge-on dish of gas and dust. The 1?1("1{ of detectable absorption implies that the density of ionized gas in the central 10 pc is less than $\sim 10^3$ cm^{-3}, assuming a temperature of $\sim 10^4$ K. The brightness of the pc-scale jets falls off rapidly on both sides of the core, suggesting that the jets are rapidly expanding during the first several pc of their travel. The rate of jet expansion must slow when the internal pressure falls below that of the external medium. We suggest that this occurs between about 10 and 200" pc from the core because the rate of decrease in radio brightness is far slower > 200 pc from the core than it is within 10 pc of the core. The position angle of the radio axis in our VLBA images agrees, within the errors, with the position angle of the VLA-scale jets. Thus there is no evidence for precession of the jets or orbital motion of the compact object at the base of the jets on time scales shorter than the material propagation time from the nucleus to the diffuse radio lobes.

Subject headings: accretion, accretion disks — galaxies: active — galaxies: individual (NGC 4261, 3C270) — galaxies: jets — galaxies: nuclei

1. Introduction

The radio source 3C270 (PKS 1216+06) associated with the E2 galaxy NGC 4261 is composed of two symmetric lobes of extended emission on opposite sides of the galaxy, connected by symmetric kiloparsec-scale jets to a compact radio source coincident with the optical nucleus of the galaxy. The compact radio core is a relatively weak VLBI source (180 mJy at 1.6 GHz; Jones, Sramek, and Terzian 1981). The radio jets extend out approximately ±4 arcmin, have opening angles of less than 5°, and are co-aligned to within 1° along position angle 88° (Birkinshaw and Davies 1985). The ratio of jet/counterjet surface brightness within a few arcseconds of the central compact source is only about 2:1, indicating that relativistic beaming effects are not strong on kpc scales. The minor axis position angle of the galaxy remains 69° ±2 over a wide range of radii (Lauer 1989b), some 1.9' from the radio axis, but the stellar rotation axis is along position angle 153° ±4 (Davies and Birkinshaw 1986) only 6° from the projected major axis of the galaxy. Evidently NGC 4261 is a nearly prolate galaxy whose stellar rotation axis has no relationship with the direction of the radio radio jets. NGC 4261 has an extremely compact optical core compared to other galaxies of similar luminosity (Lauer 1985b) and its optical brightness profile matches that of the nonisothermal core of M87 (Lauer 1985c).

Möllenhoff and Bender (1987) discovered a small dust lane in the center of NGC 4261 which is oriented perpendicular to the radio jets. More recent HST observations have revealed that the optical nucleus is surrounded by a disk of gas and dust 1.7 arcsec in diameter whose projected rotation axis is aligned within several degrees of the radio jets (Jaffe, et al. 1993; 1996). At a distance of 41 Mpc (Faber et al. 1989) the HST disk diameter is 340 pc. Some authors give distance estimates up to three times smaller than this, which of course would reduce the physical size of the HST disk by the same factor. The rotation axis of the HST disk is inclined 64° from our line of sight (Jaffe, et al. 1996),

suggesting that the radio axis may be at a similar angle from our line of sight.

The apparent inclination of the HST absorption disk and the lalgc-scale (Möllenhoff and Bender dust lane) disk differ by about 10°. It is likely that the HST disk and the larger scale dust lane are both part of a single warped disk structure (Malmabal et *al.* 1996). Since the major axis of the 11 ST disk is at a position angle of 16°, which is not orthogonal to the position angle of the radio jets, the presumed warp continues into the region close to the central black hole. Jaffe et al. (1996) point out that the apparent center of the HST disk is displaced from the optical center of the galaxy (based on isophote fitting) by at least 5 pc.

Neutral hydrogen and CO have been detected in absorption against the radio core by Jaffe and Mc Namara (1991). Their measurements indicate that the total mass of gas in the HST disk is $\sim 10^5 M_\odot$, which is sufficient to power the radio source for $\sim$ I 0^8 years. All of the above evidence suggests that the radio source is powered by material accreting in from the large-scale dust disk through the HST dust disk and eventually onto the (unseen) inner accretion disk where the radio jet formation takes place within a few Schwartzschild radii of a central massive black hole. The accreting material probably came from a merger between NGC 426 I and a smaller gas-rich galaxy. This would explain the apparently unrelated dynamics between the gas and dust in the nuclear disks and the over-all stellar dynamics of the galaxy.

We observed the nuclear region of NGC 4261 with VLBI to determine the morphology of the central radio source on parsec scales, and in particular to see if the inner radio axis remained in the same direction as the kpc-scale jets (position angle = 88°) or whether it was aligned with the apparent rotation axis of the HST disk.

2. Observations and Results

We observed NGC 4261 for 8.5 hours on 4 April 1995 using all ten antennas of the NRAO Very Long Baseline Array. Individual scans of typically 26 minutes duration were alternated between 1.6 GHz and 8.4 GHz. We recorded a bandwidth of 64 MHz with single polarization, and the data were cross-correlated on the VLBA correlator.

After cross-correlation the data were read into AIPS[1], where standard programs were used for editing, amplitude calibration, and fringe fitting. Prior to fringe fitting the strong compact radio source 1308+326 was used to derive corrections for phase slopes across the frequency channels at both 1.6 and 8.4 GHz. After fringe fitting the data were averaged over frequency and exported to the Caltech program Difmap (Shepherd, Pearson, and Taylor 1994) for additional editing, self-calibration, imaging, and deconvolution. Only marginal detections were obtained on the longest VLBA baselines (to the antennas at Saint Croix and Mauna Kea) at 1.6 GHz, but good fringes were found to all ten antennas at 8.4 GHz.

Our final VLBA images are shown in figures 1-3. Figures 1 and 2 are the full resolution images at 1.6 and 8.4 GHz, respectively. At both frequencies the source appears two-sided, although the extension to the west (the direction of the slightly brighter VLA jet) falls off somewhat more slowly in brightness than the extension to the east. In neither image does the source appear to have a one-sided "core-jet" morphology. At a distance of 41 Mpc, a milliarcsecond (mas) corresponds to 0.20 pc.

[1]The Astronomical Image Processing System was developed by the National Radio Astronomy Observatory, which is operated by Associated Universities, Inc., under a cooperative agreement with the National Science Foundation.

EDITOR: PLACE FIGURE 2 HERE

Figure 3 is an image at 8.4 GHz which was made by applying a Gaussian taper to the visibility data to match the angular resolution available at 1.6 GHz. The same field of view and restoring beam has been used for figures 2 and 3 to allow easy comparison.

EDITOR: PLACE FIGURE 3 HERE.

Although the lower resolution 8.4 GHz image appears slightly less symmetric than the full resolution version in figure 2, the source remains basically two-sided.

Attempts were made to detect more distant emission at both 1.6 and 8.4 GHz using larger image sizes and tapering the visibility data to favor short baselines. In no case did we find any emission significantly more extended than that shown in figures 1 and 3, although the range of VLBA baselines would allow more extended radio structure to be detected. We conclude that the brightness of the two parsec-scale radio jets does drop below our noise level very rapidly at both frequencies, and that this is not an artifact of the imaging procedure.

In referring to the images in figures 1-3 as symmetric or two-sided, we are implicitly assuming that the central brightness peak is the "core" of the source (the base of the radio jets). Is there any evidence to support this assumption? We have compared the images in figures 1 and 3 to determine spectral index distributions for a range of position offsets between the two images. Figure 4 shows the spectral index distribution along the east-west axis of the source when the central peaks at both frequencies are aligned. Not surprisingly, the spectral index distribution is also quite symmetric with an inverted spectrum near the center and increasingly steep spectra with increasing distance from the center. It is possible to offset the 8.4 GHz peak up to 10-12 mas from the 1.6 GHz peak without making the

spectral index $\alpha > +2.5$ (using $S_\nu \propto \nu^\alpha$), but in this case the spectral index more than ≈ 30 mas from the center becomes extremely steep ($\alpha < -2$). We therefore favor a registration in which the brightest peaks in figures 1 and 3 are nearly co-aligned, giving a spectral index distribution close to that shown in figure 4. In both morphology and spectral index distribution NGC 4261 is very similar to the parsec-scale source in Hydra A (Taylor 1996).

[EDITOR: PLACE FIGURE 4 HERE]

The surface brightness of both the east and west jets drops off rapidly at both frequencies. To quantify this, we found that all four brightness profiles could be well fit with a power law of the form (surface brightness) $\propto$ (distance from peak)^x. At 1.6 GHz the exponent x is -1.79 for the jet extending to the west and -1.95 for the jet extending to the east. Although the eastern jet fades more rapidly with distance from the core, these values are quite similar. At 8.4 GHz the corresponding exponents are x = -3.34 for the western jet and -4.02 for the eastern jet. Again, the eastern jet fades more rapidly but both values of x are similar.

The total flux density of the VLBI structure shown in figures 1 and 2 is 0.20 Jy at 1.6 GHz and 0.35 Jy at 8.4 GHz. The peak (core) surface brightness is 0.098 Jy/beam at 1.6 GHz and 0.149 Jy/beam at 8.4 GHz. This corresponds to a brightness temperature of 3.3×10^8K at 1.6 GHz and 6.2×10^8K at 8.4 GHz; these values are lower limits to the true brightness temperature of the core. The position angles at both 1.6 and 8.4 GHz are consistent with the 88° position angle of the VLA jets.

3. Discussion

It is clear from VLA images that both the east and west jet in NGC 4261 extend far beyond the scale of our VLBA images. Therefore, the disappearance of both jets within a few tens of mas of the core is not caused by their disruption or "smothering" by a dense interstellar medium. It is more likely that the jets are fading due to adiabatic expansion ('10s(" to the core. This implies that the external pressure is less than the internal jet])1"(%s(11'{'. At some point the internal pressure in the expanding jets will become lower than the external pressure (which should fall more slowly than d^{-2} at large distances), causing the opening angle of the jets to be reduced and possibly cr('still: shocks which could reaccelerate the relativistic electrons. The result will be a much slower decrease in jet brightness on kpc scales. Our angular resolution is insufficient to measure the opening angle of the pc-scale jets, but from figure 2 we can get an upper limit of approximately 10° for the east jet, compared with less than 5° on kpc scales.

We can set an upper limit on the free electron density in the inner ~ 10 pc of NGC 4261 from the apparent lack of free-free absorption at 1.6 GHz. If absorption by an inner disk or torus of ionized gas were significant, we would ('x]) ('(t to see a much more asymmetric radio morphology (*cf.* 3C84; Vermeulen, Readhead, and Backer 1994; Walker, Romney, and Benson 1994). Since both east and west jets are visible out to ~ 10 pc with similar brightness, the optical depth from free-free absorption must be much less than unity. Assuming a gas temperature of $\sim 10^4$K and a path length of 10 pc gives an electron density $< 10^3$ cm^{-3}. The total mass of ionized gas implied is $< 10^{\prime\prime\prime}$ 11,,. It appears that we have a low density, presumably hot, inner "bubble" filling the inner several pc of the nucleus (within which the radio jets expand rapidly) surrounded by a cool, higher density region (the HST absorption disk) within which the expansion of the radio jets is nearly halted.

As Bridle and Perley (1984) point out, the central brightness of an expanding

synchrotron jet decreases as a different power of distance (or radius) d depending on whether the jet is dominated by a parallel or transverse magnetic field. If equipartition is assumed, the jet brightness is proportional to $d^{-4.1}$ if $\alpha = -0.65$. This is similar to the exponents found above for both jets at 8.4 GHz (-3.3 and -4.0).

The density of free electrons in the central few pc of NGC 4261 is much lower than Levinson, Laor, and Vermeulen (1995) find for the central region of NGC 1275 (3C84), a galaxy for which there is compelling evidence for free-free absorption of radio emission at GHz frequencies from a counterjet by an obscuring disk or torus. For the disk model considered by Levinson, Laor, and Vermeulen the electron density is given by

$$n_e \approx 9\, T^{1/2}\, r^{-3/4}\, M^{1/4} \ \mathrm{cm}^{-3}$$

where T is the temperature in K, r is the path lengh in pc, and M is the mass of the presumed central black hole in units of $M_\odot$. Assuming $T \sim 10^4$K and $M \sim 10^7$ for 3C84 gives $n_e \approx (5 \times 10^4)\, r^{-3/4}$. Levinson, Laor, and Vermeulen also use a Thompson optical depth constraint to derive an upper limit of $n_e < (5 \times 10^5)\, r^{-1}$ cm^{-3}.

Taylor (1996) presents VLBA images and spectral index maps of the central radio source in Hydra A which look remarkably similar to those presented in this paper. Taylor finds evidence for significant ($\tau > 1$) free-free absorption of the radio core in Hydra A at 1.3 GHz and deduces a value of $r\, n_e^2$ which is equal to the upper limit we find for NGC 4261. At our lowest frequency of 1.6 GHz the free-free absorption deduced by Taylor would have an optical depth < 1. If the thermal gas density in the nucleus of NGC 4261 is somewhat smaller than in Hydra A, the effects of free-free absorption would be quite small at our observing frequencies. The neutral hydrogen column density in front of the radio core in NGC 4261 is approximately 20 times smaller than in Hydra A (Jaffe and McNamara 1994; Taylor 1996).

NGC 4261 contains an X-ray source whose angular extent is similar to that of the

optical galaxy (Fabbiano, Kim, and Trinchieri 1992). Einstein IPC spectra can be fit with a power law (Kim, Fabbiano, and Trinchieri 1992), but a thermal plus power law spectrum provides the best fit to ROSAT data (Worrall and Birkinshaw 1994). In the thermal plus power law model the derived neutral hydrogen column density in NGC 4261 is quite small ($N_H < 4 \times 10^{20}$ atoms cm^{-2}), and the cooling time for gas within the core radius is estimated to be 3.4×10^9 years. This is shorter than the merger age of $(8 - 10) \times 10^9$ years estimated by Schweizer and Seitzer (1992), so there may have been time for a cooling flow to begin. The angularly unresolved X-ray emission is likely to be mostly nonthermal and associated with the inner radio jet (Worrall and Birkinshaw 1994) based on the observed correlation between X-ray power law component and radio core luminosities.

There is also diffuse X-ray gas in the group containing NGC 4261 which extends to a radius of at least 40 arcmin from NGC 4261 (Davis, et al. 1995). Birkinshaw and Worrall (1994) concluded that the X-ray gas confines the kpc-scale radio jets, and that the jets terminate (flair into the two diffuse lobes) at the point where the external pressure falls below the internal pressure in the jets. This implies that the flow in the jets is slow (subsonic) and therefore that the radio source lifetime is at least 10^8 years, consistent with the merger age of Schweizer and Seitzer. The position angle of the radio axis in our VLBA images agrees, within the errors, with the position angle of the \"I,}\-scale'j('ts. Thus there is 110 evidence for precession of the jets or orbital motion of the compact object at the base of the jets 011 time scales shorter than the material propagation time from the nucleus to the diffuse radio lobes ($\gtrsim 10^8$ years). This long-term stability implies that the central compact object has a very large angular momentum.

Optical observations of the nucleus of NGC 4261 with the HST WFPC2 indicate that the ionized gas is concentrated in a region with FWHM $\approx$ 23pc, and HST FOS observations show rotational velocities which implies a central mass of (1. ? :10.4) X 10^9 hi,-. (Ford,

Ferrarese, a id Jaffe 995). The resulting mass/light ratio (V band, corrected for dust obscuratio in the nuclear disk) in the inner 20 pc exceeds 5000 in sola units, ic largest value yet determ ned in a galactic nucleus. f the centra black hole in NGC 4261 is $\sim 0^9$ $M_\odot$ it is un ikely iat i would have a ty detectable orbi al motion a bout a presumably less assive secondary nucleus from a nerger (which could be the cause of the osi ional offset between the apparent center of he I St dust disk and the radio core). In is case he secondary nucleus (and erhaps par s of the nuclear gas disk) d show almost all of he or bita motion. This could also explain the small but significant difference between the radio jet position angle and the position angle of the HST disk rotation axis.

4. Conclusions

We have found that the pc-scale radio source in the nucleus of NGC 4261 is unusually symmetric, and aligned along the same position angle as he larger-scale radio struc ure imaged with the VLA. The morphology and spectral index distribution of the pc-scale source indicates iat free-free absorption is not significant w in several pc of the radio core. The surface brightness of bot r radio jets decreases very rapidly in both directions from the core, which we iterpret as evidence for a large initial opening angle (rapid expansion). At some distance between about 50 and 500 pc ic jet opening angles decrease to the $< 5^\circ$ value seen on kpc scales. This should occur when the internal jet pressure falls elow that of the external medium.

We thank David Meier for several informative discussion about jet collimation. The Very Long Baseline Array is art of the National Radio Astronomy Observatory, which is a facility of he National Science oundation operated by Associated Universities, ic. under a coopera ive agreement with the NSF. A.W. gratefully acknowledges suppor from he

NASA Long Term Space Astrophysics Program. This research was carried out at the Jet Propulsion Laboratory, California Institute of Technology, under contract with the National Aeronautics and Space Administration.

REFERENCES

Bridle, A. 11., and Perley, R. A. 1984, ARA&A, 22, 319

Birkinshaw, M., and Davies, R. L. 1985, ApJ, 291, 32

Birkinshaw, M., and Worrall, **1).** 1994, BA AS, 26, 1504

Davies, R. L., and Birkinshaw, M. 1986, ApJ, 303, L45

Davis, D. S., Mushotzky, R. F., Mulchaey, J. S., Worrall, D. M., Birkinshaw, M., and Burstein, 1). 1995, ApJ, 444, 582

Fabbiano, G., Kim, D.-W., and Trinchieri, C. 1992, ApJ S, 80, 531

Faber, S. M., Wegner, G., Burstein, D., Davies, R. L., Dressler, A., Lynden-Bell, D., and Terlevich, R. J. 1989, ApJS, 69, 763

Ford, H., Ferrarese, L., and Jaffe, W. 1995, BA AS, 27, 1367

Jaffe, w., 1"01'(1, H.C., Ferrarese, L., vanden Bosch, F., and O'Connell, R. W. 1 993, Nature, 364, *:)1:1*

Jaffe, W., and McNamara, B. R. 1994, ApJ, 434, 110

Jaffe, W., 1"01'(1, 11., I"('I'I'al'('s('', L., vanden Bosch, I". > and O 'Connell, R. W. 1996. ApJ, 460, 214

Jones, D. L., Sramek, R. A., and Terzian, Y. 1981, ApJ, 246, 28

Kim, D.-W., Fabbiano, G., and Trinchieri, G. 1992, ApJS, 80, 645

Lauer, 'T. R. 1985a, ApJS, 57, 473

Lauer, '1'. R. 1985b, MNRAS, 216, 429

Lauer, T. R. 1985c, ApJ, 292, 104

Levinson, A., Laor, A., and Vermeulen, R. C. 1995, ApJ, 448, 589

Mahabal A Kembhavi, A., Singh, K. P., Bhat, P. N , and Prabhu, T. P. 1996, ApJ 457 598

Möllenhoff, C nd Bender, R 987, A&A, 174 63

Schweizer, F., and Seitzer, P. 992 AJ, 104, 1039

Shepherd, M ., Pearson, T. J and Taylor, G 994, BAAS, 26, 987

Taylor, G B. 1996, ApJ, in press

Vermeulen, R. C., Readhead, A C. S., and Backer D C 1994, ApJ, 430, L4

Walker, R. C., Romney, J. D and Benson, M 994 ApJ 430, 45

Worral D. M., and irkinshaw, M. 1994, ApJ, 427, 134

This manuscript was prepared with the AAS LaTeX macros v4.0.

Fig. 1. VLBA image of NGC 4261 at 1.632 GHz. The contour levels are -0. 5, -0.25, 0.25. 0.5, 1, 2, 4, 8, 16, 32, 50, 70, and 95% of the peak surface brightness (98.2 mJy/beam). The restoring beam is 14.70 x 9.1 I mas with the major axis along position angle 10.5°.

Fig. 2. Full resolution VLBA image of NGC 4261 at 8.387 GHz. The contour levels are -0.25, 0.25, 0.5, 1, 2, 5, 8, 16, 32, 50, 70, and 95% of the peak surface brightness (149.2 mJy/beam). The restoring beam is 2.69×1.56 mas with the major axis along position angle -2.2°.

Fig. 3. Low resolution VLBA image of NGC 4261 at 8.387 GHz. The contour levels are -0.12, -0.06, 0.06, 0.12, 0.25, 0.5, 1, 2, 4, 8, 16, 32, 50, 70, and 95% of the peak Sill'f:lc(' brightness (288.3 mJy/beam). For comparison with figure 1 the same field of view and restoring beam (14.70 x 9.11 mas, position angle = -10.5°) has been 11s('(1.

Fig. 4. The spectral index α between 1.6 GHz and 8.4 GHz as a function of distance along the radio axis (PA = 88°). These values were determined by aligning the brightest peak at both frequencies (see figures 1 and 3). The small peak about 32 mas east (right) of the core is caused by the knot of emission visible in the eastern jet at 8.4 GHz (see figures 2 and 3).

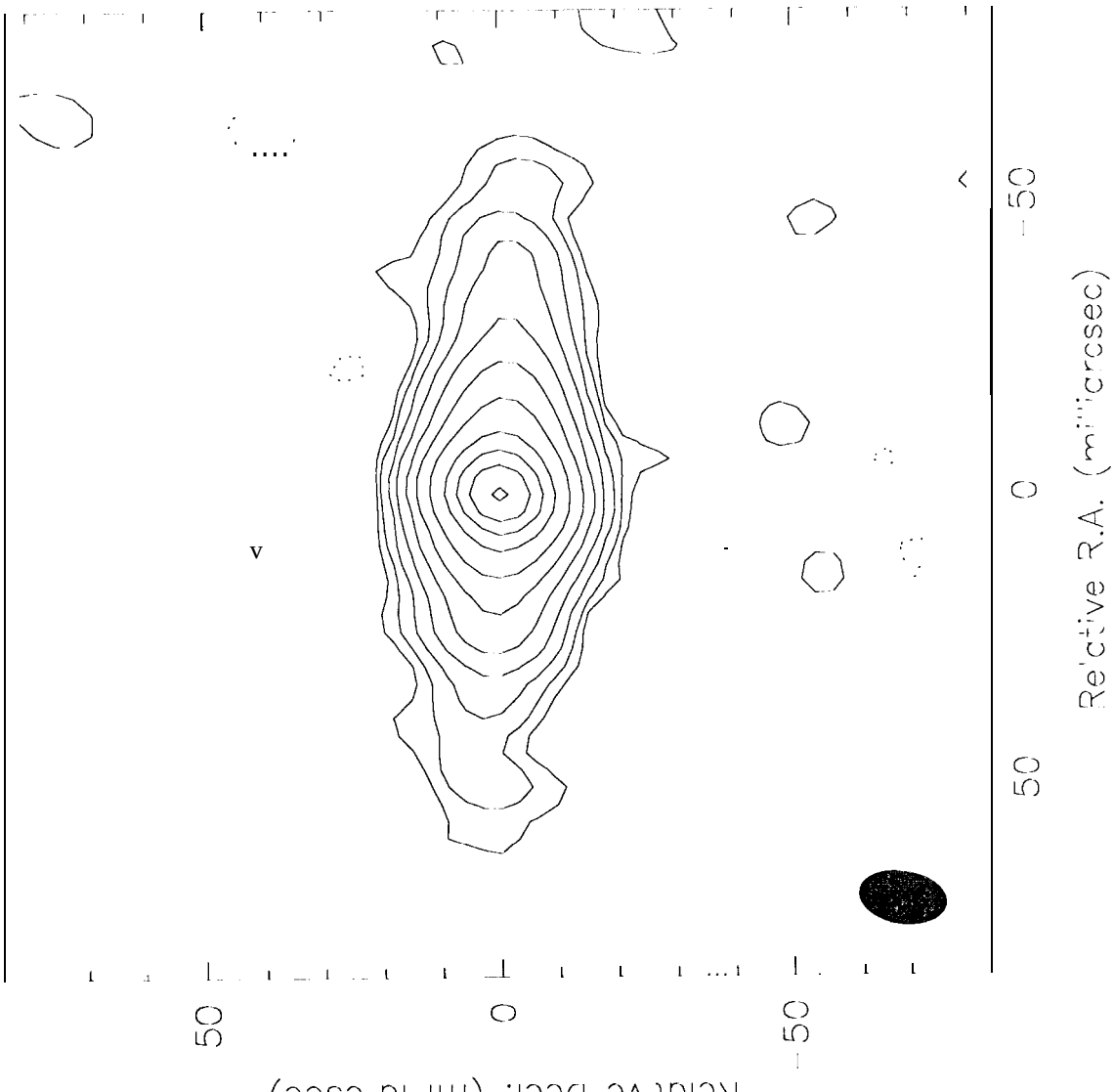
50
0
−50
Relative Dec. (milliarcsec)
50
0
−50
Relative R.A. (milliarcsec)

FIG. 1

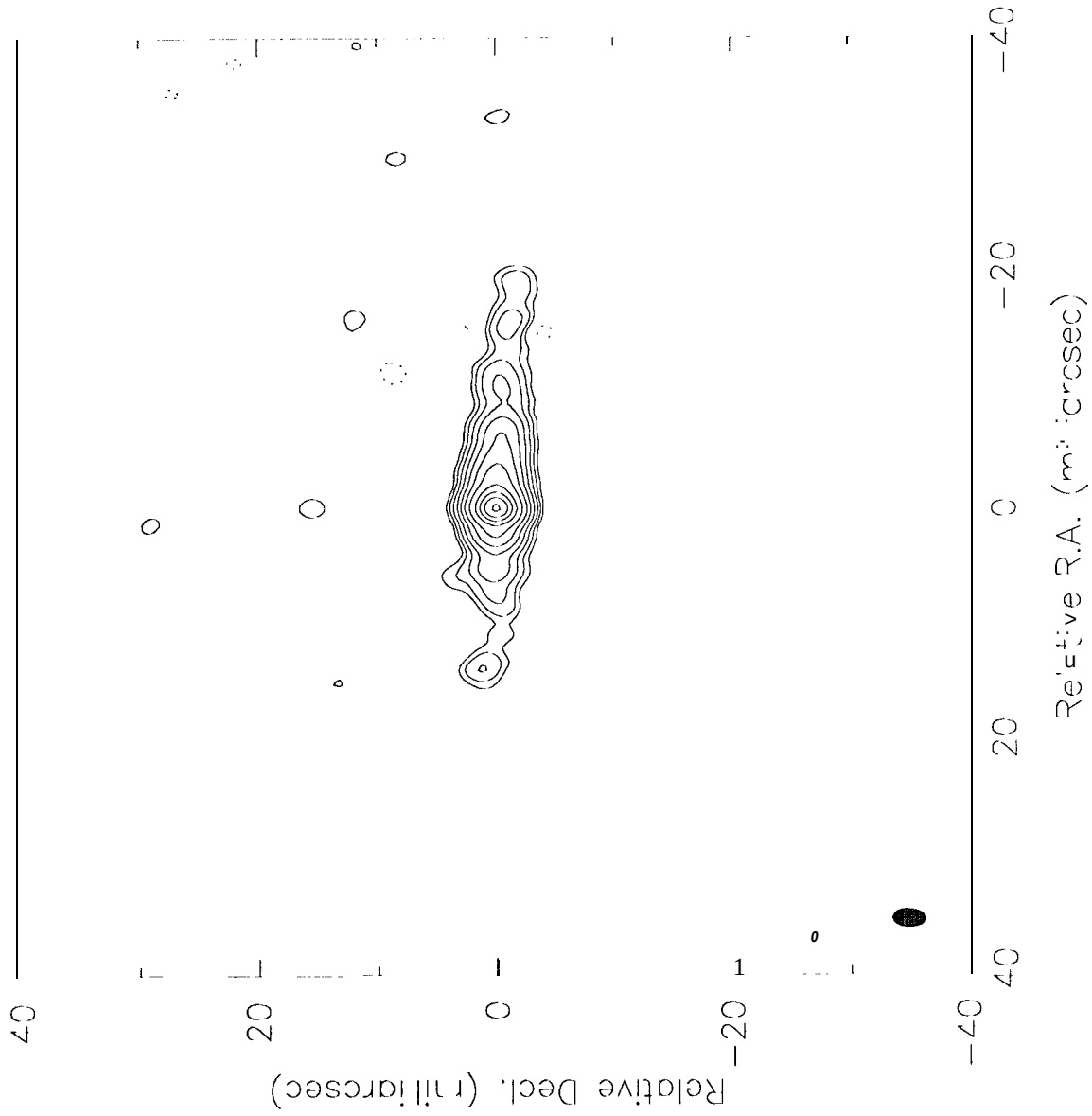
Relative Decl. (milliarcsec)
40
20
0
−20
−40
Relative R.A. (milliarcsec)
40
20
0
−20
−40

FIG. 2

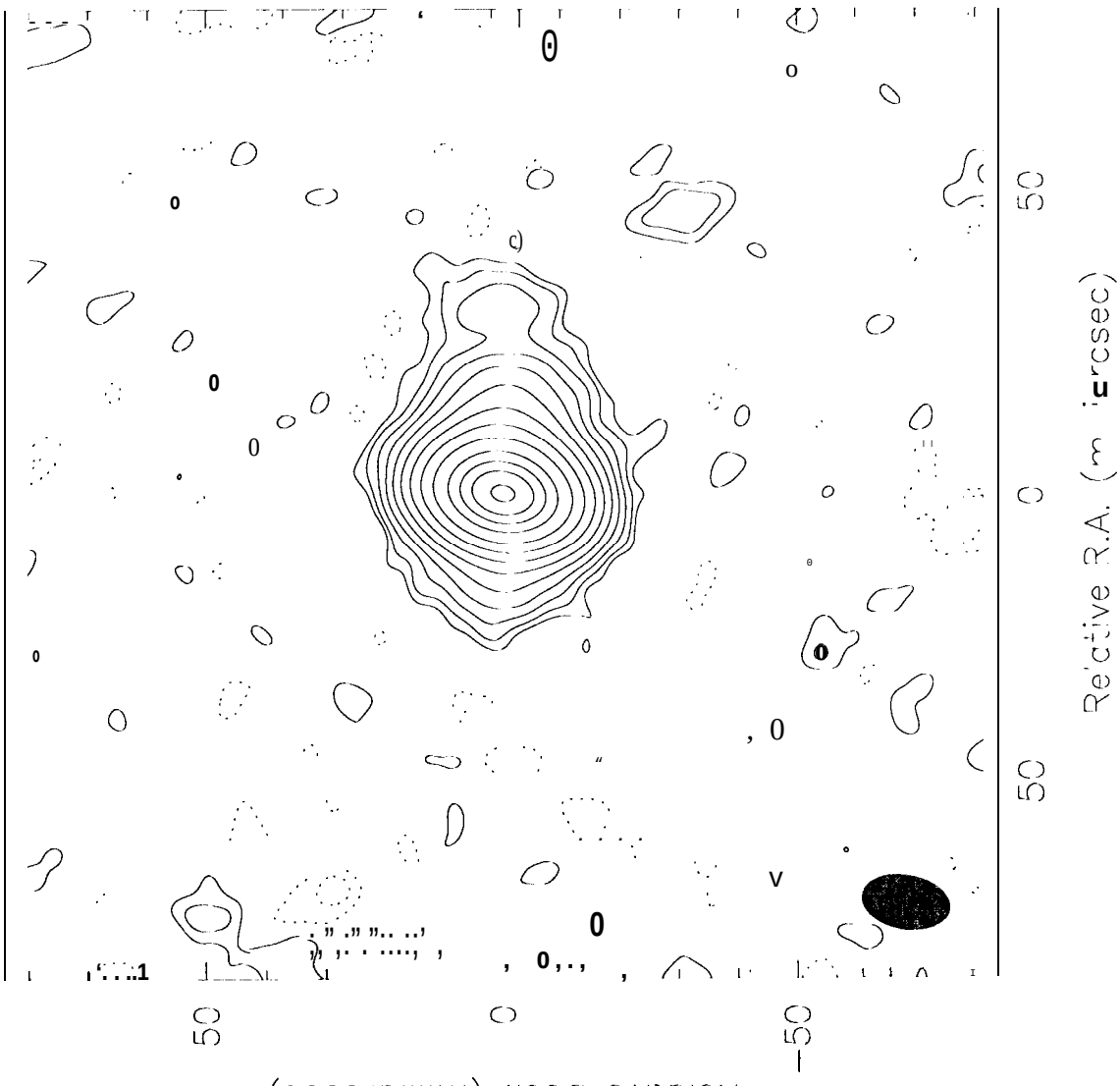
50
0
-50
Relative Decl. (milliarcsec)
50
0
-50
Relative R.A. (milliarcsec)

FIG. 3

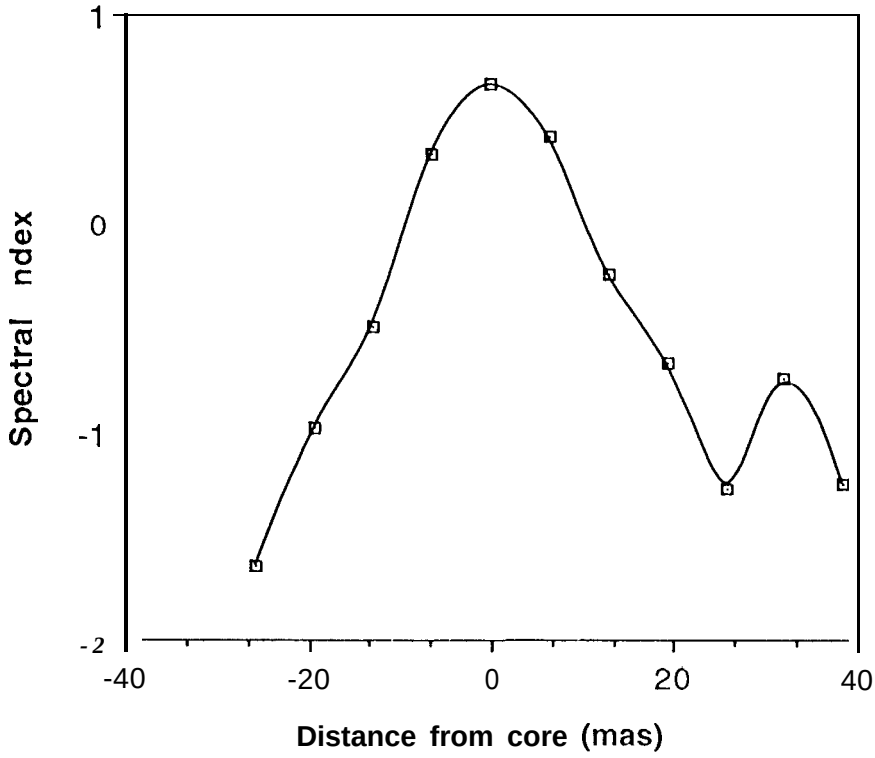

FIG. 4

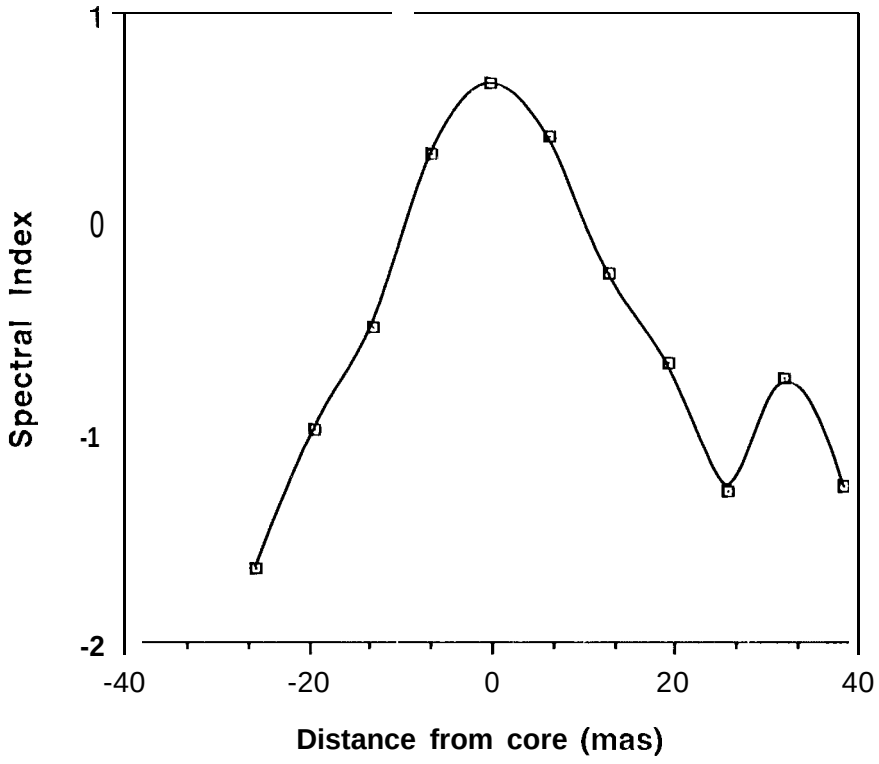

FIG. 4